

**SYNTHESIS AND CHARACTERIZATION OF PILLARED
MONOVALENT METAL ALKYL DIPHOSPHONATES**

A Senior Scholars Thesis

by

KYLEE LAUREN STOUDE

Submitted to Honors and Undergraduate Research
Texas A&M University
in partial fulfillment of the requirements for the designation as

UNDERGRADUATE RESEARCH SCHOLAR

May 2012

Major: Chemistry

**SYNTHESIS AND CHARACTERIZATION OF PILLARED
MONOVALENT METAL ALKYL DIPHOSPHONATES**

A Senior Scholars Thesis

by

KYLEE LAUREN STOUDE

Submitted to Honors and Undergraduate Research
TexasA&MUniversity
in partial fulfillment of the requirements for the designation as

UNDERGRADUATE RESEARCH SCHOLAR

Approved by:

Research Advisor:
Associate Director, Honors and Undergraduate Research:

Abraham Clearfield
Duncan MacKenzie

May 2012

Major: Chemistry

ABSTRACT

Synthesis and Characterization of Pillared Monovalent Metal Alkyl Diphosphonates.
(May 2012)

Kylee Lauren Stouder
Department of Chemistry
Texas A&M University

Research Advisor: Dr. Abraham Clearfield
Department of Chemistry

A particular type of organic-inorganic hybrid materials is represented by the metal organophosphonates in which phosphonate groups are bonded to the metal backbone. The metal phosphonates of general composition $X[\text{HO}_3\text{PC}_4\text{H}_8\text{PO}_3\text{H}_2]$, $X[\text{HO}_3\text{PC}_5\text{H}_{10}\text{PO}_3\text{H}_2]$, and $X[\text{HO}_3\text{PC}_6\text{H}_{12}\text{PO}_3\text{H}_2]$, where $X = \text{K}, \text{Rb}, \text{Cs}$, have been synthesized by microwave reactions to study the effect of both the change in the size of the metal and the length of the ligand on the three-dimensional structure. Structural studies from single crystal X-ray diffraction data reveal that these compounds exhibit a 1:2 metal to phosphonate ratio, making them Brønsted acids; this 1:2 ratio is uncommon in metal diphosphonates but has been observed in a few other structures including the alkali metal ethylene and biphenylenediphosphonates. All structures in our study formed pillared materials with distinct organic and inorganic layers. Compounds of the potassium series were found to be isostructural, while more variation was found within the structures of the rubidium and cesium series. Structural variation within the compounds can be attributed to increasing the length of the ligand alkyl chain as well as

increasing the size of the metal cation. It was our hope that extending the length of the alkyl chain would afford increased porosity relative to the previously synthesized ethylene diphosphonates. Structural and other physical trends exhibited by our compounds can potentially be applied to future work on di- and tri-valent metal diphosphonates, which are more difficult to structurally characterize due to poor crystallization.

ACKNOWLEDGMENTS

I am extremely grateful for the continued support of the Texas A&M Undergraduate Research program as well as the Texas A&M Department of Chemistry and the Dr. Clearfield research group. Dr. Clearfield has been wonderful to work for. I could not have asked for a better mentor and boss. I am also extremely thankful to my graduate research mentor, Tiffany Kinnibrugh. In the last year and a half that I have been working with her she has taught me so much and been extremely patient with me as I learn. Working in the Dr. Clearfield research group has truly been a blessing.

I also greatly appreciate the generous support of the Robert A. Welch Foundation (Grant A-0673) and the National Science Foundation (Grant DMR-0652166) which helps make this research possible.

TABLE OF CONTENTS

	Page
ABSTRACT	iii
ACKNOWLEDGMENTS.....	v
TABLE OF CONTENTS	vi
LIST OF FIGURES.....	vii
CHAPTER	
I INTRODUCTION.....	1
II METHODS.....	4
Synthesis of the ligands alkyl diphosphonates	4
Synthesis of pillared monovalent metal alkyl diphosphonates	6
Characterization of compounds.....	9
III RESULTS.....	10
Crystal structure descriptions	11
IV DISCUSSION	24
V CONCLUSIONS.....	28
REFERENCES.....	29
CONTACT INFORMATION	30

LIST OF FIGURES

FIGURE	Page
1 General reaction scheme for ligand synthesis	4
2 General reaction scheme for synthesis of pillared materials	7
3 View of coordination sphere (top left, 3A) and metal framework (bottom left, 3B) of compound 1a viewed along the <i>c</i> -axis and crystal packing (right, 3C) of compound 1a viewed along the <i>a</i> -axis.....	12
4 View of coordination sphere (top left, 4A) and metal framework (bottom left, 4B) of compound 1b viewed along the <i>c</i> -axis and crystal packing (right, 4C) of compound 1b viewed along the <i>a</i> -axis.....	14
5 View of coordination sphere (top left, 5A) and metal framework (bottom left, 5B) of compound 1c viewed along the <i>c</i> -axis and crystal packing (right, 5C) of compound 1c viewed along the <i>a</i> -axis.....	15
6 View of coordination sphere (top left, 6A) and metal framework (bottom left, 6B) of compound 2b viewed along the <i>a</i> -axis and crystal packing (right, 6C) of compound 2b viewed along the <i>c</i> -axis.....	17
7 View of coordination sphere (top left, 7A) and metal framework (bottom left, 7B) of compound 2c viewed along the <i>c</i> -axis and crystal packing (right, 7C) of compound 2c viewed along the <i>b</i> -axis.....	18
8 View of coordination sphere (top left, 8A) and metal framework (bottom left, 8B) of compound 3a viewed along the <i>c</i> -axis and crystal packing (right, 8C) of compound 3a viewed along the <i>a</i> -axis.....	20
9 View of coordination sphere (top left, 9A) and metal framework (bottom left, 9B) of compound 3b viewed along the <i>a</i> -axis and crystal packing (right, 8C) of compound 3b viewed along the <i>c</i> -axis.....	21

- 10 View of coordination sphere (top left, 10A) and metal framework (bottom left, 10B) of compound 3c viewed along the *a*-axis and crystal packing (right, 10C) of compound 3c viewed along the *c*-axis.....23
- 11 Structures of K (left), Rb (center), and Cs (right) ethylene diphosphonates.³....25
- 12 View of un-distorted (left) compared to distorted (right) alkyl chain of butylene diphosphonates26

CHAPTER I

INTRODUCTION

Metal phosphonate chemistry, which had its beginning in 1978, involves the bonding of phosphonate groups to metal atoms resulting in one-, two-, and three-dimensional materials that have promise as robust porous solids. The first series was synthesized using zirconium as the metal forming a layered structure.¹ Since then the use of mono-, di-, tri-, and tetra-valent metals has been widely explored. These structures exhibit several potential applications including use as catalysts², sorbents, ion exchangers³, and sensors.⁴

In previous research monovalent metal phenylphosphonates⁵, ethylenediphosphonates², methylenediphosphonates⁶, and biphenylenebisphosphonates⁷ have been synthesized and characterized using Li, Na, K, Rb, and Cs as the metal ions. For all these compounds a one to two metal to phosphonate ratio was obtained causing three of the original four phosphonic acid protons to be retained, which makes them Brønsted acids. In these materials, the structure has an influence on the accessibility of the acidic protons. For the case of the monovalent metal phenylphosphonates where the compounds form layers, intercalation of both ammonium ions and amines occurred. Here an increase in *d*-spacing is observed with increase in amine size suggesting that the layers move apart

This thesis follows the style of *Journal of the American Chemical Society*.

to accommodate the amines.⁵ All of the diphosphonates formed three dimensional structures therefore porosity must be inherent to the structure in order to intercalate amines.^{2,5} For the more flexible ligands intercalation of ammonium ions occurred, while for monovalent metal biphenylenediphosphonates no porosity was found from surface area measurements. Access to the protons in these materials is blocked but if it could be made porous, it too would have potential as a Bronsted acid catalyst. In fact, recent research has been done to increase the access to acidic protons by addition of amines as a structure directing agent. The downfall in this approach is the removal of the amine can be difficult to accomplish.

Our interest lies in whether the porosity of these materials could be increased by altering the ligand. One possible means of doing this would be to increase the length of the alkyl chain of the ligand. Monovalent metal alkylphosphonates have been synthesized and characterized for the ligands methylenebisphosphonate (C1) and 1,2-ethylenebisphosphonate (C2)^{5,2}; however perhaps by using 1,3-propanebisphosphonate (C3), 1,4-butanebisphosphonate (C4), 1,5-pentanebisphosphonate(C5), and 1,6-hexanebisphosphonate(C6) the porosity of the structure would be increased due to their flexibility. Furthermore, we wish to investigate the effect of increasing metal cation size on structure. In previous syntheses metal ion size seems to contribute to variation in structure and coordination of the inorganic framework. The structure of the inorganic framework plays an indirect role in the porosity of the compounds. For instance, in the

monovalent metal ethylene bisphosphonates a decrease in porosity was observed with increasing metal ion size.²

CHAPTER II

METHODS

All commercially available reactants (Li_2CO_3 99.1% Fisher, $\text{Na}_2\text{CO}_3 \cdot \text{H}_2\text{O}$ 99.5% Baker Analyzed, K_2CO_3 99% Sigma Aldrich, Rb_2CO_3 99% Alfa Aesar, and Cs_2CO_3 99% Alfa Aesar, Triisopropyl phosphate Sigma Aldrich, 1,4 dibromobutane, 1,5 dibromopentane and 1,6 dibromohexane Sigma Aldrich) were used as purchased without further purification unless specified.

Synthesis of the ligands alkyl diphosphonates

The ligands alkyl diphosphonates were synthesized using the Arbuzov reaction according to previous methods.⁸ A general reaction scheme is shown in Figure 1.

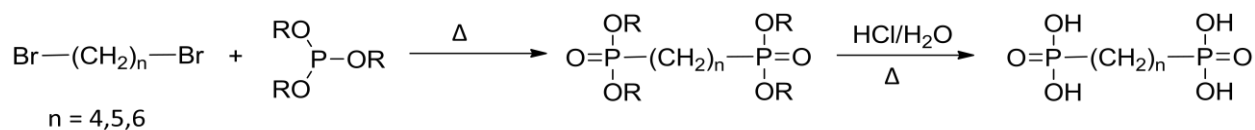


Figure 1. General reaction scheme for ligand synthesis.

Preparation of 1,4-butanebisphosphonic acid: $H_2O_3PC_4H_8PO_3H_2$

Triisopropylphosphite (0.20 mol, 46.0 mL) and 1,4-dibromobutane (.069 mol, 8.3 mL) were added to a roundbottom flask and heated, with stirring, at 120 °C in an oil bath overnight. The solution was distilled at 120 °C. Deionized water (60 mL) and concentrated hydrochloric acid (60 mL) were added and the solution was heated at 110°C for 1 day. The solution was concentrated using rotary evaporation, leaving yellow-tinted oil. The product was washed with acetone (~25 mL) and then dried, forming a white powder (6.897 g, 46.32% yield).

Preparation of 1,5-pentanebisphosphonic acid: $H_2O_3PC_5H_{10}PO_3H_2$

Triisopropylphosphite (0.20 mol, 46.0 mL) and 1,5-dibromopentane (.069 mol, 9.2 mL) were added to a roundbottom flask and heated, with stirring, at 120 °C in an oil bath overnight. The solution was distilled at 120 °C. Deionized water (60 mL) and concentrated hydrochloric acid (60 mL) were added and the solution was heated at 110°C for 1 day. The solution was concentrated using rotary evaporation, leaving yellow-tinted oil. The product was washed with acetonitrile and white solid was isolated through vacuum filtration (9.98 g, 61.7% yield).

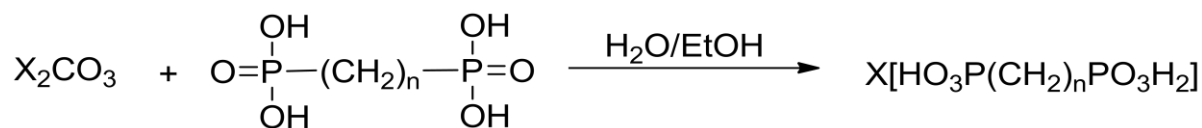
Preparation of 1,6-hexanebisphosphonic acid: $H_2O_3PC_6H_{12}PO_3H_2$

Triisopropylphosphite (0.20 mol, 46.0 mL) and 1,6-dibromohexane (.069 mol, 10.4 mL) were added to a roundbottom flask and heated, with stirring, at 120 °C in an oil bath

overnight. The solution was distilled at 120 °C. Deionized water (60 mL) and concentrated hydrochloric acid (60 mL) were added and the solution was heated at 110°C for 1 day. The solution was concentrated using rotary evaporation, leaving yellow-tinted oil. The product was washed with acetonitrile and white solid was isolated through vacuum filtration (3.01 g, 17.88 % yield). Low yield was a result of multiple unsuccessful attempts to purify the compound.

Synthesis of pillared monovalent metal alkyl diphosphonates

All pillared materials were synthesized via microwave reaction using an CEM Explorer® 12 Hybrid microwave. A general reaction scheme is shown in Figure 2. The solvent system was adjusted for each compound; it was found that each compound required slightly different conditions for crystallization. All crystals were obtained from slow evaporation of solvent, as the compounds were found to be very soluble and did not yield solid product after heating. Hydrothermal reactions were attempted as an alternative synthetic route. All hydrothermal reactions also required slow evaporation. Due to an increased amount of solvent needed to perform hydrothermal reactions relative to microwave reactions this synthetic method was abandoned. Single crystals were obtained from slow evaporation and used in single crystal x-ray diffraction experiments. Bulk reactions contained impurities which were most likely starting materials, but purification is difficult because the starting materials and pillared compounds have similar solubilities.



X= K, Rb, Cs
n= 4,5,6

Figure 2. General reaction scheme for synthesis of pillared materials.

Microwave synthesis of compound 1a: $K(\text{HO}_3\text{PC}_4\text{H}_8\text{PO}_3\text{H}_2)$

Reactions with a 1:1 ratio of 1,4-butanebisphosphonate (0.4587 mmol, 0.1000 g) and potassium carbonate (0.4587 mmol, 0.0634 g) were heated at 145°C in 1 mL of 1:1 water to ethanol mixture for 7 hrs. Single crystals were obtained through slow evaporation at room temperature over a period of approximately 4 weeks.

Microwave synthesis of compound 1b: $K(\text{HO}_3\text{PC}_5\text{H}_{10}\text{PO}_3\text{H}_2)$

Reactions with a 1:1 ratio of 1,5-pentanebisphosphonate(0.4312 mmol, 0.1000g) and potassium carbonate (0.4312 mmol, 0.0596g) were heated at 145 °C in 1 ml of 2:1 water:ethanol mixture for 7 hrs. Single crystals were obtained through slow evaporation at room temperature over a period of approximately 4 weeks.

Microwave synthesis of compound 1c: $K(HO_3PC_6H_{12}PO_3H_2)$

Reactions with a 1:1 ratio of 1,6-hexanebisphosphonate (0.4065 mmol, 0.1000 g) and potassium carbonate (0.4065 mmol, 0.0596 g) were heated at 145 °C in 1 ml of 1:3 water to ethanol mixture for 7 hrs. Single crystals were obtained through slow evaporation at room temperature over a period of approximately 4 weeks.

Microwave synthesis of compound 2b: $Rb(HO_3PC_5H_{10}PO_3H_2)$

Reactions with a 1:1 ratio of 1,5-pentanebisphosphonate(0.2155 mmol, 0.0500g) and rubidium carbonate (0.2155 mmol, 0.0498 g) were heated at 145°C in 1 ml of 1:1 water:ethanol mixture for 7 hrs. Single crystals were obtained through slow evaporation at room temperature over a period of approximately 4 weeks

Microwave synthesis of compound 2c: $Rb(HO_3PC_6H_{12}PO_3H_2)$

Reactions with a 1:1 ratio of 1,6-hexanebisphosphonate (0.0813 mmol, 0.0200g) and rubidium carbonate (0.0813 mmol, 0.0188 g) were heated at 145°C in 1 ml of 3:1 water:ethanol mixture for 7 hrs. Single crystals were obtained through slow evaporation at room temperature over a period of approximately 4 weeks.

Microwave synthesis of compound 3a: $Cs(HO_3PC_4H_8PO_3H_2)$

Reactions with a 1:1 ratio of 1,4-butanebisphosphonate (0.4587 mmol, 0.1000g) and cesium carbonate (0.4587 mmol, 0.1495 g) were heated at 145°C in 1 ml of 1:1

water:ethanol mixture for 7 hrs. Single crystals were obtained through slow evaporation at room temperature over a period of approximately 4 weeks.

Microwave synthesis of compound 3b: Cs(HO₃PC₅H₁₀PO₃H₂)

Reactions with a 1:1 ratio of 1,5-pentanebisphosphonate (0.2155 mmol, 0.0500g) and cesium carbonate (0.2155 mmol, 0.0702 g) were heated at 145°C in 1 ml of 1:1 water:ethanol mixture for 7 hrs. Single crystals were obtained through slow evaporation at room temperature over a period of approximately 4 weeks.

Microwave synthesis of compound 3c: Cs(HO₃PC₆H₁₂PO₃H₂)

Reactions with a 1:1 ratio of 1,6-hexanebisphosphonate (0.2033mmol, 0.0500g) and cesium carbonate (0.2033 mmol, 0.0662 g) were heated at 145°C in 1 ml of 2:1 water:ethanol mixture for 7 hrs. Single crystals were obtained through slow evaporation at room temperature over a period of approximately 4 weeks.

Characterization of compounds

Powder XRD patterns were recorded using a Bruker D8-Focus Bragg-Brentano X-ray powder diffractometer (Cu K α radiation, $\lambda=1.54178$ Å) operating at room temperature. Single crystal data were collected on a Bruker-AXS Apex II CCD X-ray diffractometer (Mo K α radiation, $\lambda= 0.71073$ Å) operating at 110 K.

CHAPTER III

RESULTS

Eight monovalent metal diphosphonates, $K(HO_3PC_4H_8PO_3H_2)$, $K(HO_3PC_5H_{10}PO_3H_2)$, $K(HO_3PC_6H_{12}PO_3H_2)$, $Rb(HO_3PC_5H_{10}PO_3H_2)$, $Rb(HO_3PC_6H_{12}PO_3H_2)$, $Cs(HO_3PC_4H_8PO_3H_2)$, $Cs(HO_3PC_5H_{10}PO_3H_2)$, and $Cs(HO_3PC_6H_{12}PO_3H_2)$, have been synthesized and structurally characterized. Structural studies from single crystal X-ray diffraction data reveal that these compounds exhibit a 1:2 metal to phosphonate ratio. This results in retention of 3 of the 4 acidic protons, making the compounds Brønsted acids. The 1:2 ratio is uncommon in metal diphosphonates but has been observed in a few other structures including the alkali metal ethylene² and biphenylene-diphosphonates.⁷ All compounds form three dimensional pillared materials in which the inorganic framework is bound to the diphosphonate alkyl chains to form distinct inorganic and organic layers. Potassium butane-, pentane-, and hexane- as well as rubidium hexane- bisphosphonates were found to have isostructural inorganic frameworks. Greater variation is seen within the structures of the remaining rubidium and cesium compounds. The ligands butane-, pentane-, and hexane- bisphosphonate will be referred to as C4, C5, and C6, respectively.

Crystal structure descriptions

When considering bond distance, the maximum Van der Waal's radii were considered⁹. This is consistent with structural determinations of the ethylenediphosphonates². Bond distances are presented in Table 1.

Table 1. M-O Bond Distances (Å) of Alkali Metal Alkyl Diphosphonates

	K-C4	K-C5	K-C6		Rb-C5		Rb-C6		Cs-C4		Cs-C5		Cs-C6
K1-O1	2.79(2)	2.8746(17)	2.805(19)	Rb1-O1	2.940(3)	Rb1-O1	2.955(6)	Cs1-O1	3.177(3)	Cs1-O1	3.066(2)	Cs1-O1	3.18(1)
K1-O2	2.85(2)	2.8871(17)	2.904(2)	Rb1-O1(b)	2.938(3)	Rb1-O2	3.016(6)	Cs1-O1(b)	3.111(3)	Cs1-O1(b)	3.078(2)	Cs1-O1(b)	3.13(1)
K1-O2(b)	2.97(3)	2.9480(18)	2.976(2)	Rb1-O2	2.952(3)	Rb1-O2(b)	3.070(6)	Cs1-O2	3.185(3)	Cs1-O2	3.2067(19)	Cs1-O2	3.20(1)
K1-O3	2.64(2)	2.7728(18)	2.697(2)	Rb1-O3	2.993(3)	Rb1-O3	2.862(6)	Cs1-O3	3.366(3)	Cs1-O3	3.143(2)	Cs1-O3	3.36(1)
K1-O4	2.95(2)	2.8871(17)	2.915(19)	Rb1-O4	2.988(3)	Rb1-O4	3.024(6)	Cs1-O4	3.203(4)	Cs1-O4	3.2253(19)	Cs1-O4	3.24(1)
K1-O4(b)	2.95(3)	2.9480(18)	2.959(2)	Rb1-O5	2.975(3)	Rb1-O4(b)	3.058(6)	Cs1-O4(b)	3.123(3)	Cs1-O5	3.444(2)	Cs1-O4(b)	3.14(2)
K1-O5	2.80(2)	2.8746(17)	2.813(2)			Rb1-O5	2.976(6)	Cs1-O5	3.358(3)	Cs1-O5(b)	3.149(2)	Cs1-O5	3.35(1)
K1-O6	2.77(2)	2.7728(18)	2.744(2)			Rb1-O6	2.908(6)	Cs1-O6	3.119(3)			Cs1-O6	3.14(2)

Crystal structure of compound 1a: $K(HO_3PC_4H_8PO_3H_2)$

Each potassium atom is coordinated to eight oxygen atoms to form a dodecahedron with an average K-O bond distance of 2.840 Å. The maximum value of the K-O bond distance is 2.970 Å. Each potassium atom is bonded to six different phosphate moieties,

thus two chelations are observed. The oxygen atoms O(1) and O(2) chelate through the phosphorus atom P(2). The oxygen atoms O(4) and O(5) chelate through the phosphorus atom P(1). The oxygen atoms O(2) and O(4) also donate to neighboring potassium atoms. Both chelations are oriented along the same plane, and the third oxygen on either phosphorus bridges to the neighboring potassium atom along the *ab*-diagonal. The diphosphonates link the inorganic layers to form a pillared structure. The inorganic layers are separated by a distance of 10.90 Å and are stacked along the *c*-axis. Slight distortion is observed in the alkyl chain of the diphosphonate ligand. The crystal structure can be seen in Figure 3.

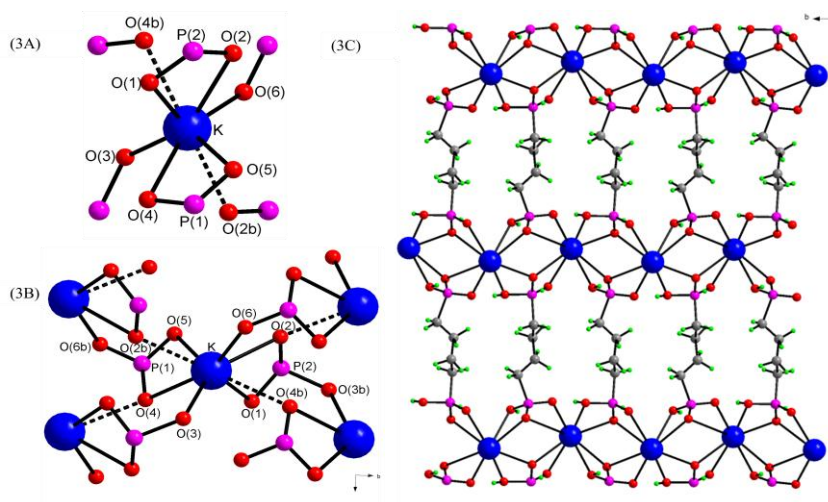


Figure 3. View of coordination sphere (top left, 3A) and metal framework (bottom left, 3B) of compound 1a viewed along the *c*-axis and crystal packing (right, 3C) of compound 1a viewed along the *a*-axis.

Crystal structure of compound 1b: $K(HO_3PC_5H_{10}PO_3H_2)$

Each potassium atom is coordinated to eight oxygen atoms to form a dodecahedron with an average K-O bond distance of 2.871 Å. The maximum value of the K-O bond distance is 2.948 Å. Each potassium atom is bonded to six different phosphate moieties, thus two chelations are observed. The oxygen atoms O(1) and O(2) chelate through the phosphorus atom P(2). The oxygen atoms O(4) and O(5) chelate through the phosphorus atom P(1). The oxygen atoms O(2) and O(4) also donate to neighboring potassium atoms. Both chelations are oriented along the same plane, and the third oxygen on either phosphorus bridges to the neighboring potassium atom along the *ab*-diagonal. The diphosphonates link the inorganic layers to form a regular pillared structure. The inorganic layers are separated by a distance of 12.22 Å and are stacked along the *c*-axis. The crystal structure can be seen in Figure 4.

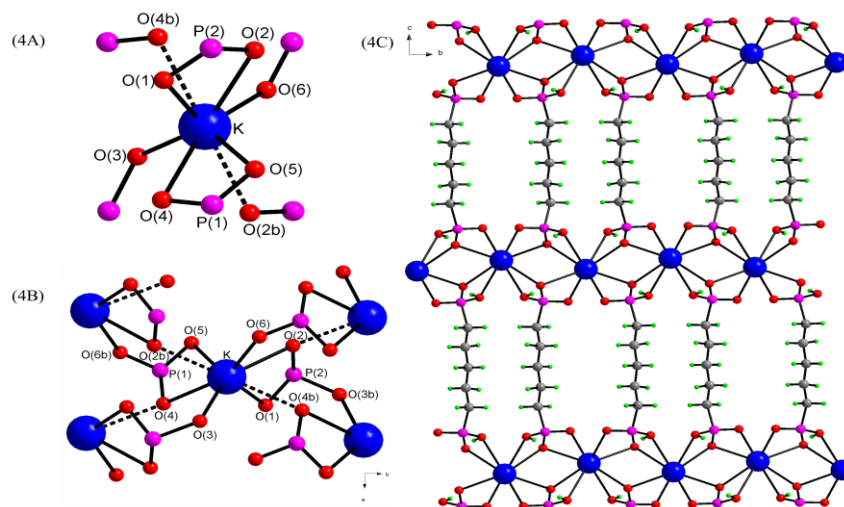


Figure 4. View of coordination sphere (top left, 4A) and metal framework (bottom, left, 4B) of compound 1b viewed along the *c*-axis and crystal packing (right, 4C) of compound 1b viewed along the *a*-axis.

Crystal structure of compound 1c: $K(HO_3PC_6H_{12}PO_3H_2)$

Each potassium atom is coordinated to eight oxygen atoms to form a dodecahedron with an average K-O bond distance of 2.852 Å. The maximum value of the K-O bond distance is 2.976 Å. Each potassium atom is bonded to six different phosphate moieties, thus two chelations are observed. The oxygen atoms O(1) and O(2) chelate through the phosphorus atom P(2). The oxygen atoms O(4) and O(5) chelate through the phosphorus atom P(1). The oxygen atoms O(2) and O(4) also donate to neighboring potassium atoms. Both chelations are oriented along the same plane, and the third oxygen on either phosphorus bridges to the neighboring potassium atom along the *ab*-

diagonal. The diphosphonates link the inorganic layers to form a pillared structure. The inorganic layers are separated by a distance of 13.31 Å and are stacked along the *c*-axis. Slight distortion is observed in the alkyl chain of the diphosphonate ligand. The crystal structure can be seen in Figure 5.

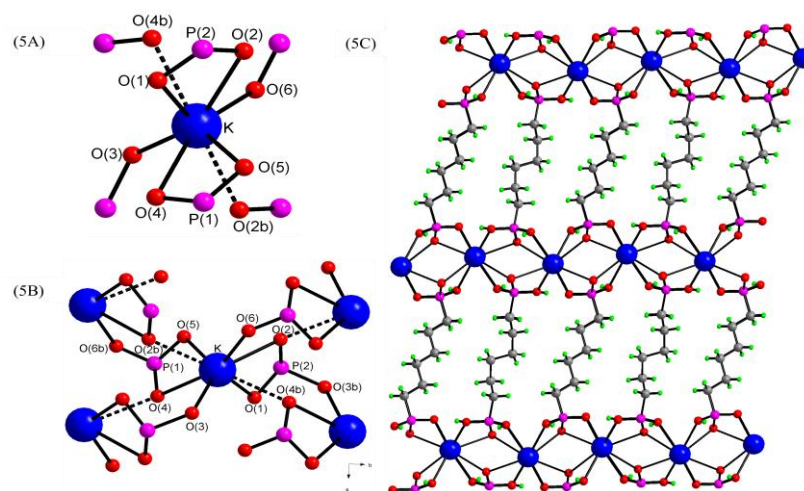


Figure 5. View of coordination sphere (top left, 5A) and metal framework (bottom left, 5B) of compound 1c viewed along the *c*-axis and crystal packing (right, 5C) of compound 1c viewed along the *a*-axis.

Crystal structure of compound 2b: Rb(HO₃PC₅H₁₀PO₃H₂)

Each rubidium atom is coordinated to six oxygen atoms with an average Rb-O bond distance of 2.964 Å. The maximum value of the Rb-O bond distance is 2.993 Å. Each rubidium atom exhibits one chelation and is thus bonded to five different phosphate moieties. The oxygen atoms O(1) and O(2) chelate through the phosphorus atom P(1). The oxygen atom O(1) also donates to a neighboring rubidium atom in the *c*-direction and the oxygen atom O(3) bridges to a neighboring rubidium atom. The second phosphate moiety bridges two neighboring rubidium atoms, through O(4)-P(2)-O(5), in the *c*-direction. This bridging combined with the donation of the oxygen atom O(1) results in the formation of chains, linking adjacent rubidium atoms in the *c*-axis. These chains are linked together through the bridging of the oxygen atom O(3). The oxygen atom O(6) is non-bonding. The diphosphonates link the inorganic layers to form a pillared structure. The organic layers appear to cross when viewed along the *c*-axis. The inorganic layers are separated by a distance of 12.71 Å and are stacked along the *a*-axis. Alternate chains in the *a*-axis cross each other. The crystal structure can be seen in Figure 6.

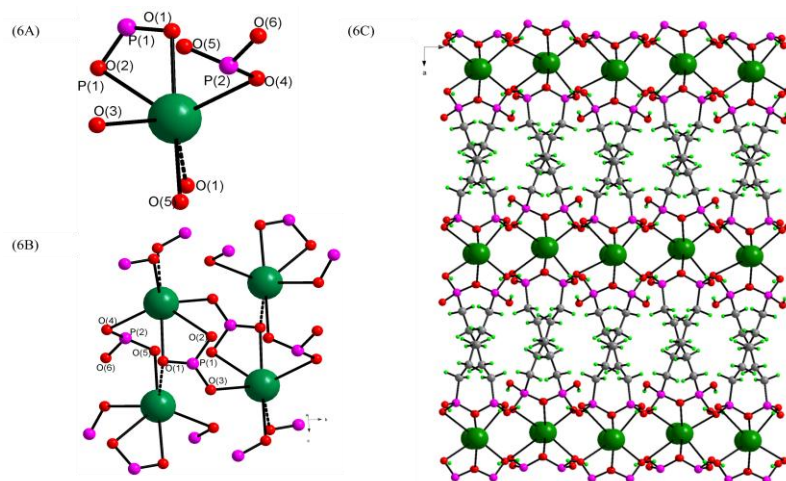


Figure 6. View of coordination sphere (top left, 6A) and metal framework (bottom left, 6B) of compound 2b viewed along the *a*-axis and crystal packing of compound 2b (right, 6C) viewed along the *c*-axis.

Crystal structure of compound 2c: $Rb(HO_3PC_6H_{12}PO_3H_2)$

Each rubidium atom is coordinated to eight oxygen atoms to form a dodecahedron with an average Rb-O bond distance of 2.984 Å. The maximum value of the Rb-O bond distance is 3.070 Å. Each rubidium atom is bonded to six different phosphate moieties, thus two chelations are observed. The oxygen atoms O(1) and O(2) chelate through the phosphorus atom P(2). The oxygen atoms O(4) and O(5) chelate through the phosphorus atom P(1). The oxygen atoms O(2) and O(4) also donate to neighboring rubidium atoms. Both chelations are oriented along the same plane, and the third oxygen on either phosphorus bridges to the neighboring rubidium atom. The diphosphonates

link the inorganic layers to form a pillared structure. The inorganic layers are separated by a distance of 13.96 Å and are stacked along the *c*-axis. Slight distortion is observed in the alkyl chain of the diphosphonate ligand. The crystal structure can be seen in Figure 7.

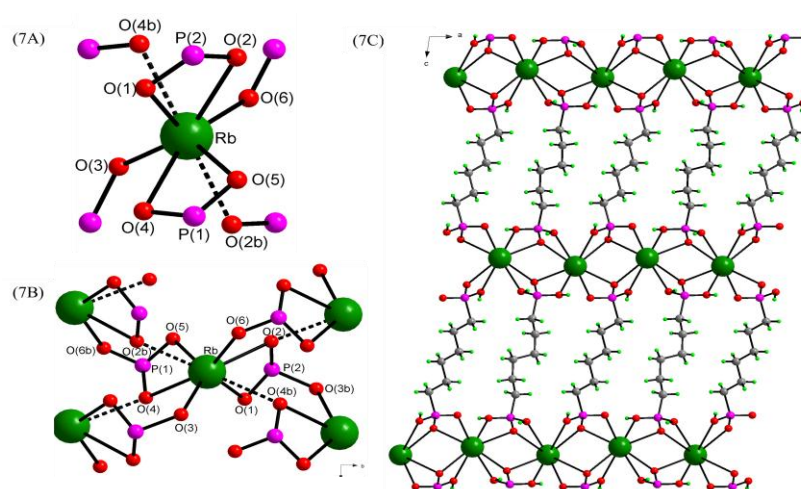


Figure 7. View of coordination sphere (top left, 7A) and metal framework (bottom left, 7B) of compound 2c viewed along the *c*-axis and crystal packing of compound 2c (right, 7C) viewed along the *b*-axis.

Crystal structure of compound 3a: Cs(HO₃PC₄H₈PO₃H₂)

Each cesium atom is coordinated to eight oxygen atoms, forming a dodecahedron, with an average Cs-O bond distance of 3.205 Å. The maximum value of the Cs-O bond distance is 3.366 Å. Each cesium atom exhibits two chelations and is thus bonded to six different phosphate moieties. Both chelations run along the *ac*- plane. The oxygen atoms O(1) and O(2) chelate through the phosphorus atom P(1) and the oxygen atoms O(4) and O(5) chelate through the phosphorus atom P(2). The oxygen atoms O(2) and O(5) both donate to neighboring cesium atoms to form four membered chains that link neighboring cesium atoms in the *b*-direction. The inorganic layer is built from linking the chains through both the donation of the oxygen atoms O(1) and O(4) and by bridging of the oxygen atoms O(3) and O(6), which link to adjacent cesium atoms. The diphosphonates link the inorganic layers to form a pillared structure. The inorganic layers are separated by a distance of 11.89 Å and are stacked along the *c*-axis. The crystal structure can be seen in Figure 8.

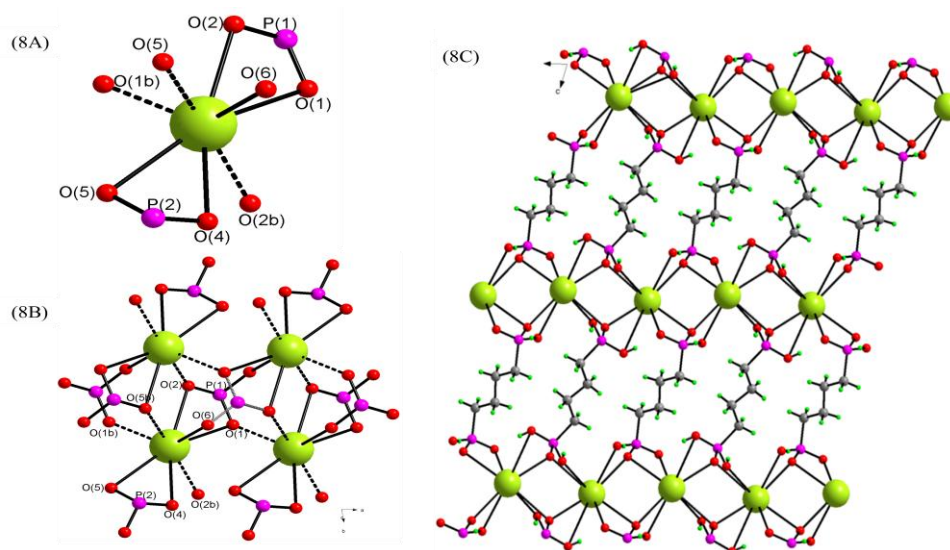


Figure 8. View of coordination sphere (top left, 8A) and metal framework (bottom left, 8B) of compound 3a viewed along the *c*-axis and crystal packing (right, 8C) of compound 3a viewed along the *a*-axis.

Crystal structure of compound 3b: Cs(HO₃PC₅H₁₀PO₃H₂)

Each cesium atom is coordinated to seven oxygen atoms with an average Cs-O bond distance of 3.187 Å. The maximum value of the Cs-O bond distance is 3.444 Å. Each cesium atom exhibits two chelations and is thus bonded to five different phosphate moieties. The oxygen atoms O(1) and O(2) chelate through the phosphorus atom P(1), and the oxygen atoms O(4) and O(5) chelate through the phosphorus atom P(2). The oxygen atoms O(1) and O(5) also donate to neighboring cesium atoms to form

fourmembered rings which link neighboring cesium atoms in the c -direction forming chains. The oxygen atom O(3) bridges these chains together to form the inorganic layer. The oxygen atom O(6) is non-bonding. The diphosphonates link the inorganic layers to form a pillared structure. The organic layers appear to cross when viewed along the c -axis. The inorganic layers are separated by a distance of 12.896 Å and are stacked along the a -axis. The crystal structure can be seen in Figure 9.

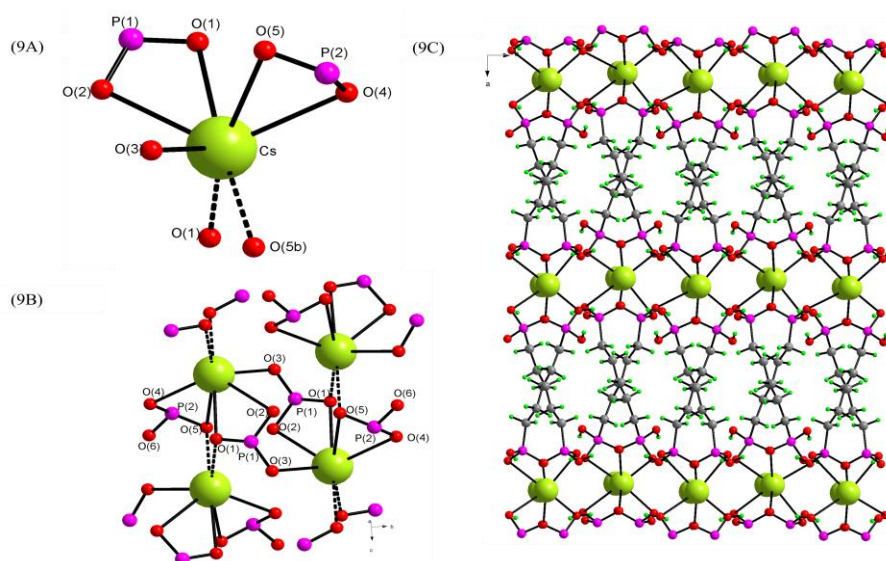


Figure 9. View of coordination sphere (top left, 9A) and metal framework (bottom left, 9B) of compound 3b viewed along the a -axis and crystal packing (right, 9C) of compound 3b viewed along the c -axis.

Crystal structure of compound 3c:Cs(HO₃PC₆H₁₂PO₃H₂)

Each cesium atom is coordinated to eight oxygen atoms, forming a dodecahedron, with an average Cs-O bond distance of 3.218 Å. The maximum value of the Cs-O bond distance is 3.360 Å. Each cesium atom exhibits two chelations and is thus bonded to six different phosphate moieties. Both chelations run along the *ac*- plane. The oxygen atoms O(1) and O(2) chelate through the phosphorus atom P(1) and the oxygen atoms O(4) and O(5) chelate through the phosphorus atom P(2). The oxygen atoms O(2) and O(5) both donate to neighboring cesium atoms to form four membered chains that link neighboring cesium atoms in the *b*-direction. The inorganic layer is built from linking the chains through both the donation of oxygen atoms O(1) and O(4) and by bridging of the oxygen atoms O(3) and O(6), which link to adjacent cesium atoms. The diphosphonates link the inorganic layers to form a pillared structure. The inorganic layers are separated by a distance of 14.37 Å and are stacked along the *c*-axis. The crystal structure can be seen in Figure 10.

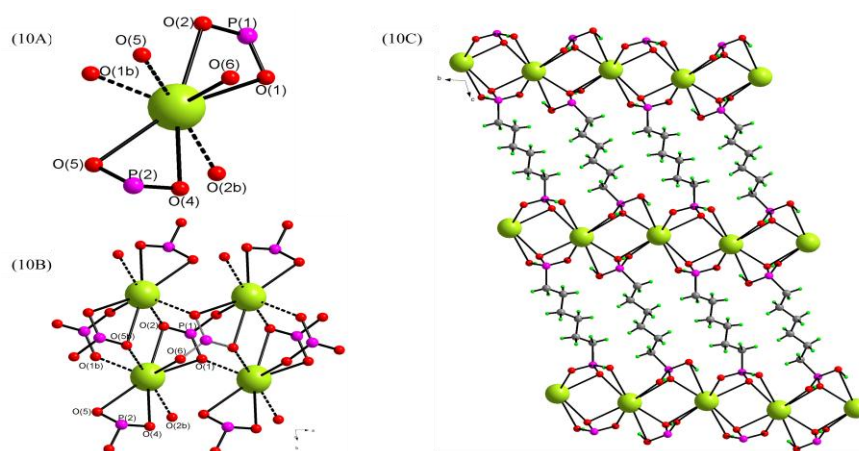


Figure 10. View of coordination sphere (top left, 10A) and metal framework (bottom left, 10B) of compound 3c viewed along the *a*-axis and crystal packing (right, 10C) of compound 3c viewed along the *a*-axis.

CHAPTER IV

DISCUSSION

This project set out to study the structural effects of increasing the alkyl chain length of a diphosphonate ligand in a series of monovalent metal pillared structures. The structural diversity of the compounds 1a-3c reflects changes in the alkyl chain length and metal ion size. These compounds exhibit several interesting trends which can be attributed to one or both of the above mentioned variables.

The profound difference between these structures and the previously reported ethylenediphosphonates² is the formation of distinct organic and inorganic layers. This layering is not observed in the potassium, rubidium, or cesium ethylenediphosphonates² (Figure 11). The formation of distinct layers can be attributed to the longer butane, pentane, and hexane alkyl chains. These longer four, five and six carbon chains prevent bonding between metal atoms of different layers; whereas the shorter ethylene chain allows this type of interaction.

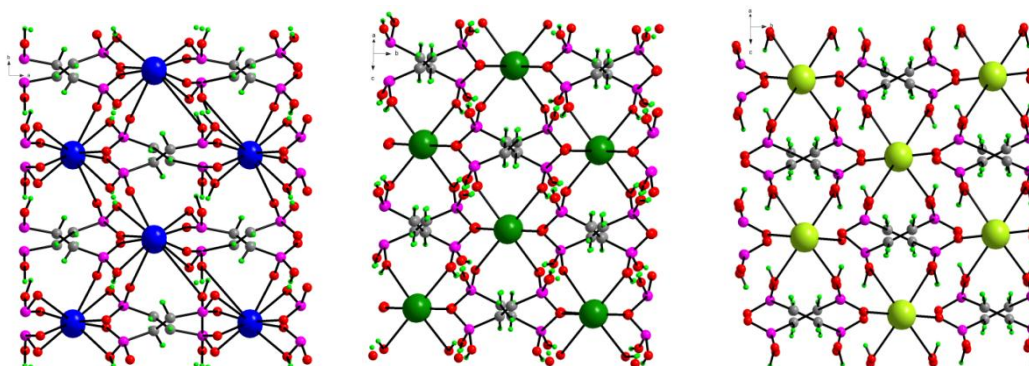


Figure 11. Structures of K (left), Rb (center), and Cs (right) ethylene

diphosphonates²

Little structural diversity is seen within the potassium series. All compounds appear to be isostructural with regard to their metal framework and differ only in their interlayer spacing (a result of increasing the alkyl chain length of the ligand). Each potassium ion has a coordination of eight, forming a dodecahedron. Each atom also forms two chelations and is thus bridged to six neighboring potassium ions.

A change in structure is seen in the C5 series from the potassium atom to the rubidium and cesium atoms. In the rubidium and cesium structures the alkyl chains, rather than running straight along a single axis as is observed in compound 1b (Figure 2C), run along a diagonal and appear to criss-cross when these structures are viewed along the *c*-axis (Figure 4C and Figure 7C). This is most likely attributed to the increase in metal ion size from potassium to rubidium and cesium atoms.

The cesium and rubidium compounds are structurally more diverse than the potassium compounds. This diversity is seen in both the inorganic and organic layers. For both the cesium and rubidium series a change in coordination is seen from the C5 to C6 series. All metal atoms, with the exception of those in compounds 2b and 3b, are eight-coordinate. In compound 2b rubidium is six-coordinate, and in compound 3b cesium is seven-coordinate. This coordination allows, as previously mentioned, criss-crossing of the alkyl chains in compounds 2b and 3b. The C4 and C6 rubidium and cesium compounds are more similar to the potassium series in that their alkyl chains do not exhibit this crossed formation. Interestingly, 2c is isostructural with the potassium series.

An interesting trend is noted in the compounds with even numbered alkyl chains (C4 and C6). The alkyl chain of these compounds adopts a distorted, higher energy conformation (Figure 12).

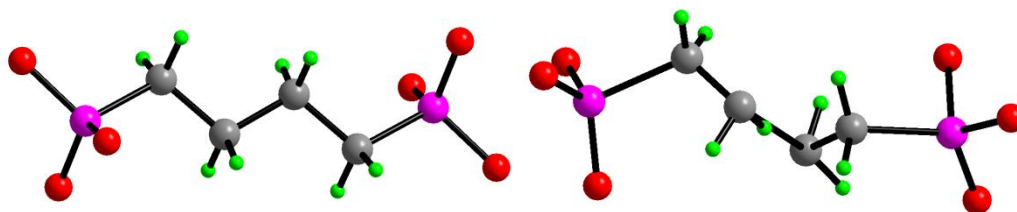


Figure 12. View of un-distorted (left) compared to distorted (right) alkyl chain of butylene diphosphonates.

This is not observed in any compounds of the C5 series. The distortion seems to be necessary in order to accommodate bonding to the inorganic framework. Interestingly the distortion disappears as the size of the metal cation increases and is not seen in any compounds of the cesium series. The cesium compounds appear to allow the lower energy conformation by slight slanting of the inorganic framework to relieve the strain in the alkyl chain.

CHAPTER V

CONCLUSIONS

Several general trends were observed in the C4, C5, and C6 monovalent metal diphosphonates. Potassium metal formed compounds with isostructural inorganic frameworks, while the rubidium and cesium series formed a more diverse range of structures. Structural differences are also seen between even and odd alkyl chains with increase in cation size from potassium. However, an increase in metal cation size seems to decrease distortion of chains with even numbers of carbons.

Future work with these compounds will include completion of single crystal structure determination for remaining compounds in the series, including all compounds in the lithium and sodium series as well as rubidium C4. Synthesis and characterization of bulk products will also be performed as well as possible amine intercalation to determine if the acidic hydrogen atoms are accessible.

REFERENCES

- (1) Zhang, B., Clearfield, A. *J. Amer. Chem. Soc.* **1979**, *119*, 2751.
- (2) Rao K.P., Vidyassagar, K. *Acta Cryst.* **2005**, *61*, 1794-1796.
- (3) Moller, T., Bestaoui, N., Wierzbicki, M., Adams, T., Clearfield, A. *Applied Radiation and Isotopes*. **2011**, *69*, 947-954.
- (4) Jayswal, A., Chudasama, U. *Acta Chem. Slovenica* **2007**, *54*, 654-660.
- (5) Rao K.P., Vidyassagar K. *Eur. J. Inorg. Chem.* **2005**, 4936-494.
- (6) Rao K.P., Vidyassagar K. *Eur. J. Inorg. Chem.* **2006**, 813-819.
- (7) Kinnibrugh, T.L., Garcia, N., Clearfield, A. *J. Solid State Chem.* **2012**, *187*, 149-158.
- (8) Bhattacharya, A.K., Thyagarajan, G. *Chem. Rev.* **1981**, *81*, 415-430.
- (8) Shannon, R.D. *Acta Cryst.* **1976**, *32*, 751-767.

CONTACT INFORMATION

Name: Kylee Lauren Stouder

Professional Address: c/o Dr. Abraham Clearfield
Department of Chemistry
MS 4227
Texas A&M University
College Station, TX 77843

Email Address: ky.st27@tamu.edu

Education: B.A., Chemistry, Texas A&M University, May 2013
Magna Cum Laude
Undergraduate Research Scholar